J. Fluid Mech. (1996), *vol.* 323, *pp.* 79–105

Axisymmetric swirling flow around a vortex breakdown point

By ZVI RUSAK

Department of Mechanical Engineering, Aeronautical Engineering and Mechanics, Rensselaer Polytechnic Institute, Troy, NY 12180-3590, USA

(Received 24 April 1995 and in revised form 1 April 1996)

The structure of an axisymmetric and inviscid swirling flow around a vortex breakdown point is analysed. The model assumes that a free axisymmetric bubble surface is developed in the flow with a stagnation point at its nose. The classical Squire–Long equation for the stream function $\psi(x, y)$ (where $y = r^2/2$) is transformed into a free boundary problem for the solution of $y(x, \psi)$. The development of the flow is studied in three regions: the approaching flow ahead of the bubble, around the bubble nose and around the separated bubble surface. Asymptotic expansions are constructed to describe the flow ahead of and behind the stagnation point in terms of the radial distance from the vortex axis and from the bubble surface, respectively. In the intermediate region around the stagnation point, the flow is approximated by an asymptotic series of similarity terms that match the expansions in the other regions. The analysis results in two possible matching processes. Analytical expressions are given for the leading term of the intermediate expansion for each of these processes. The first solution describes a swirling flow around a constant-pressure bubble surface, over which the flow is stagnant. The second solution represents a swirling flow around a pressure-varying bubble surface, where the flow expands along the bubble nose. In both solutions, the bubble nose has a parabolic shape, and both exist only when $H' > 0$ (where H' is the derivative at the vortex centre of the total head H with the stream function ψ, and can be determined from the inlet conditions). This result is shown to be equivalent to Brown & Lopez's (1990) criterion for vortex breakdown. Good agreement is found in the region around the stagnation point between the pressure-varying bubble solution and available experimental data for axisymmetric vortex breakdown.

1. Introduction

1.1. *Review*

High-Reynolds-number swirling flows are characterized by abrupt changes and regions of flow reversal and instabilities known as the vortex breakdown phenomena. The continuing research toward understanding these phenomena has been strongly motivated by their significant harmful effects on slender aircraft configurations flying at high angles of attack. However, for confined swirling flows through pipes or in closed containers, it may have potential technological applications like flame stabilization in combustion chambers. Vortex breakdown phenomena can also occur in flows in hydrocyclon separators as well as in swirling jets behind nozzles, and are also common to the motion of atmospheric vortices such as tornados. Therefore, the ability to understand the complicated structures that develop as a consequence of vortex breakdown and to predict the flow conditions that lead to these phenomena is

essential for the future utilization of swirling flows in the design of advanced aerodynamic configurations, combustion chambers, nozzles, and other flow devices where swirl has a dominant influence.

The vortex breakdown phenomena have been widely studied and several review papers on this subject have been presented, including the reports by Hall (1972), Leibovich (1978, 1984) and Escudier (1988). Although there has been extensive research, the fundamental nature of these phenomena remains largely unexplained.

Experimental results from vortex flows around highly swept sharp-edged wings at high angles of attack and vortex flows in tubes show several distinct forms of vortex breakdown (Sarpkaya 1971, 1974; Faler & Leibovich 1977; Bruecker & Althaus 1992, 1995). They range from various helical disturbances to a spiral type breakdown or a strong, nearly axisymmetric, bubble type. The various types of breakdown can develop in flows with the same Reynolds number, with only a small change in the swirl ratio (ratio of circumferential speed to axial speed) of the flow. The breakdown phenomenon is characterized by an abrupt change in the flow above a certain swirl ratio. A stagnation point suddenly emerges in the free swirling flow, followed by regions of flow reversals and turbulence behind it. The experimental results of Faler & Leibovich (1978), Uchida, Nakamura & Ohsawa (1985) and Bruecker & Althaus (1995) on axisymmetric bubble breakdown show that the axial flow along the vortex core centreline rapidly decelerates to stagnation as a linear function of the distance from the stagnation point. Also, regarding circumferential velocity profiles, the angular velocity along the axis decreases toward the breakdown point, and swirl strongly deviates from solid-body rotation at the stagnation point.

Numerical simulations of vortex flows using the Navier–Stokes or the Euler equations have recently made some progress and describe flow fields that resemble vortex breakdown (Leibovich & Kribus 1990; Beran & Culick 1992; Spall, Gatski & Ash 1990; Spall & Gatski 1991; Brewer 1991; Lopez 1990, 1994). The various types of vortex breakdown can be simulated, depending on the initial disturbances, the upstream (or inlet) conditions and, specifically, the boundary conditions along the outer lateral boundaries of the computational domain.

The theoretical analyses of the vortex breakdown phenomena have suggested three basic different classes of explanations: the critical-state concept, the analogy to boundary-layer separation, and hydrodynamic instabilities. The critical-state theory (Benjamin 1962) relates the characteristics of a swirling columnar flow to the ability of the flow to sustain standing, axisymmetric small-disturbance waves. Supercritical vortex flows have low swirl ratios and are unable to support such waves, while subcritical flows have high swirl ratios and are able to sustain standing waves. Benjamin (1962) described the axisymmetric breakdown in a rather simple model as a transition from an upstream supercritical flow to a downstream subcritical flow; however, the relevance of this model to the vortex breakdown is not yet clear. Leibovich & Kribus (1990) showed that small-amplitude axisymmetric standing waves tend to blow up near the critical state and stationary axisymmetric solitary waves are formed which may describe an axisymmetric bubble and can exist only in a supercritical flow.

The analogy to flow separations (Hall 1972) is based on the failure of the quasi-cylindrical approximations to the Navier–Stokes equations to describe a swirling flow with large streamwise gradients. The topology of the flow near the breakdown point changes drastically and looks similar to the separation of a boundary layer over a rigid wall (Spall & Gatski 1991). Trigub (1985) analysed the singularity in the solution of the quasi-cylindrical equations and showed that the radial velocity tends to grow to infinity

as the stagnation point is approached. Similar evidence was found in recent calculations by Beran & Culick (1992). However, Trigub's (1985) analysis is limited to flows with relatively small swirl of the order of $1/Re_c^{1/2}$ (where Re_c is the Reynolds number based on the viscous core radius), whereas in experiments the swirl is much larger. The failure of the quasi-cylindrical approximation is not yet fully understood.

The stability analyses study the tendency of small disturbances imposed on a vortex flow to grow or decay in time and space. The analyses of Lessen, Singh & Paillet (1974) and Leibovich & Stewartson (1983) define several criteria for the stability of a vortex flow to general three-dimensional axisymmetric and non-axisymmetric perturbations. It is found that a columnar vortex with a large rotational core (the 'Q-vortex' model) is stable to axisymmetric perturbations when the swirl ratio is greater than 0.403, but it is unstable to non-axisymmetric helical perturbations when the swirl ratio is less than about 1.6. A review of vortex stability criteria is given in Leibovich (1984). It is important to note that the relation between vortex breakdown and vortex stability is yet unclear. As was pointed out by Leibovich (1984), breakdown can occur in a vortex flow with just a little sign of instability and a vortex flow can become unstable without any breakdown phenomena.

Leibovich (1984) has proposed a theoretical scenario to explain the onset of breakdown in a vortex flow in a tube. It is suggested that several interacting mechanisms are involved: the axisymmetric, bubble-type breakdown phenomenon is associated with the development of large-amplitude axially symmetric waves in a basic supercritical vortex flow, which are equilibrated by energy transfer to non-axisymmetric instabilities of modest amplitude and are also affected by axial variations caused by pressure gradients along the vortex core. This hypothesis is based on the weakly nonlinear 'trapped wave' theory of Randall & Leibovich (1973) and recent solutions for the development in space and time of large-amplitude axially symmetric solitary waves on columnar vortices (Leibovich & Kribus 1990; Kribus & Leibovich 1994). However, the interaction among the various mechanisms remains a complicated open problem to study. Some support for this model may be found in the calculations by Beran & Culick (1992). However, the continuation method of the flow into the separation zone in Leibovich & Kribus (1990) raises some difficulties. It is not clear whether analytical continuation of the circulation and total head functions into the bubble zone is the preferred model to use in the inviscid framework.

In another approach, Escudier & Keller (1983) and Keller, Egli & Exley (1985) described the axisymmetric breakdown as a two-stage transition around a semi-infinite stagnation zone of free boundaries. Their solution matches between a given inlet columnar flow condition and another outlet columnar flow solution that has the same flow force. However, this solution clearly is limited only to a certain swirl ratio of the inlet flow which is at a supercritical stage. This solution was not extended to other swirl ratios with a fixed vortex core radius.

Several criteria have recently been proposed to predict the onset of breakdown in a vortex flow. Spall, Gatski & Grosch (1987) suggested a criterion for the breakdown of vortex flows in tubes in terms of the local Rossby number (the inverse of swirl ratio) of the flow, that is defined at the radial distance of maximum swirl velocity. Based on previous experimental, numerical and theoretical studies, they found that for any Reynolds number greater than 100, vortex breakdown occurs only when the local Rossby number of the upstream flow is less than a critical value – about 0.65.

Brown & Lopez (1990) analysed the Euler equations that describe an incompressible and inviscid axisymmetric swirling flow and proposed a theoretical criterion for the axisymmetric breakdown that is based on the generation of negative azimuthal

vorticity on some stream surfaces in the flow. It relates the tangents of the helix angles α_0 and β_0 for the velocity and vorticity vectors at an upstream station. A stagnation point will appear in the flow only when the condition $\alpha_0 > \beta_0$ is satisfied. This idea showed good agreement with numerical results of vortex breakdown in tubes.

Brown & Lopez (1990) also suggested a positive feedback mechanism between the divergence of the stream function surfaces and the development of negative azimuthal vorticity in the vortex core for the generation of a separation zone in a swirling flow. This mechanism shows good agreement with numerical simulations and with the experimental results of Bruecker & Althaus (1995).

Lundgren & Ashurst (1989) and Marshall (1991) studied area-varying waves on curved vortex tubes by using a Polhausen type of integral momentum approach. The vortex breakdown is described as a 'shock jump' in the vortex flow across which the core radius and the circulation of the vortex can be discontinuous. Theoretical criteria for both stationary axisymmetric and helical breakdowns were presented in terms of the local swirl ratio of the flow.

Recently, Goldshtik & Hussain (1992) have presented the idea of the development of internal stagnation zones in inviscid vortical flows as a basic model to explain the vortex breakdown phenomenon. They have analysed the various possibilities of the continuation of a vortical incompressible flow into internal separation regions that may develop in a swirling flow. Formal analytical continuation may lead to swirl reversals that are physically unlikely to occur. The inviscid-limit solution of the axisymmetric Navier–Stokes equations suggests an internal flow with no swirl and a linear change of the azimuthal vorticity with the radius. Such a solution may lead to matching problems with the flow outside the separation region. It has also been shown that separation zones will appear in axisymmetric swirling flows above a critical value of the swirl ratio due to the spatial instability of the flow to azimuthal vorticity disturbances. The model of a stagnation zone describes the flow inside the bubble with no swirl and no azimuthal vorticity. It is also a specific inviscid-limit solution and has been suggested by Goldshtik & Hussain (1992) as the preferred model to describe the axisymmetric bubble-type breakdown. Observations (Uchida *et al.* 1985) show that within the bubble there is a very slow motion compared to the outer flow. It should also be mentioned that the theory of Escudier & Keller (1983) described the axisymmetric breakdown as a transition around a stagnation zone of free boundaries. However, the existence, uniqueness and stability of stagnation zones in vortical axisymmetric flows has not been studied yet and it still remains an open problem to investigate.

The review of the theoretical and numerical studies on vortex breakdown shows that this phenomenon remains largely unexplained, specifically with regard to the details of the swirling flow around the stagnation point, the shape of the separation zones and the conditions for its existence.

1.2. *Model assumptions*

This paper concentrates on the nearly axisymmetric vortex breakdown phenomenon and the flow structure near the nose of the bubble. Experiments on swirling flows in a pipe (Sarpkaya 1971, 1974, 1995; Faler & Leibovich 1977, 1978; Uchida *et al.* 1985; Escudier 1984; Bruecker & Althaus 1992, 1995; Bruecker 1995) provide insight into the structure and stability of the nearly axisymmetric vortex breakdown phenomenon. In all of the cases the inlet flow to the pipe, the flow near the inlet decelerating to stagnation and expanding around the nose of the bubble, and most of the bubble envelope, all show a high degree of axial symmetry (Faler & Leibovich 1977). Non-axisymmetric perturbations develop mostly near the rear end of the bubble, inside the

bubble and downstream in the wake of the bubble and are mostly confined to those regions. The flow inside the recirculation bubble zone is very complicated. Some experiments show that there is an inclined toroidal vortex ring near the downstream end of the recirculation bubble, which gyrates at a regular frequency about the axis of the tube and is accompanied by the loss of axisymmetry near the rear end of the bubble (Sarpkaya 1971, 1974, 1995; Bruecker & Althaus 1992; Bruecker 1995). Other experiments, however (Faler & Leibovich 1978; Uchida *et al.* 1985), show the generation of two vortex rings inside the bubble which preserves the axisymmetry of the flow. It can also be observed (see figure 8*c* from Sarpkaya 1995; figure 4 from Bruecker & Althaus 1992 and figures 3, 4 and 6*b* from Faler & Leibovich 1977) that even downstream of the bubble nose but outside the bubble and its wake, the flow preserves a degree of axisymmetry. Also, inside the bubble the flow is relatively slow and so the transfer of momentum and kinetic energy from the inside of the bubble to its surroundings is relatively small. The recent experiments of Bruecker & Althaus (1995) are the only ones known that describe the evolution in time of the breakdown. They show that the bubble evolves in time with a strong axisymmetry (see figures 1 and 5 in Bruecker & Althaus 1995). They also show that it is only after the axisymmetric bubble has been formed that asymmetric disturbances in the wake of the bubble may slightly change the flow structure inside the bubble (see figure 5 in Bruecker & Althaus 1995) but a high degree of symmetry is kept. Bruecker & Althaus (1995) also indicated that Sarpkaya (1971, 1974) had observed a more asymmetric bubble-type breakdown than those they found.

Therefore, it may be concluded that the non-axisymmetric perturbations observed develop from a base axisymmetric flow that contains a separation zone and to the leading order the bubble and the flow around the bubble are axisymmetric. This is also the reason why most of the theoretical and numerical approaches to the nearly axisymmetric vortex breakdown phenomenon have concentrated on studying the axisymmetric case (theoretical approaches: Benjamin 1962; Hall 1972; Randall & Leibovich 1973; Keller & Egli 1985; Escudier 1988; Leibovich & Kribus 1990; Brown & Lopez 1990; Berger & Erlebacher 1995; numerical approaches: Grabowski & Berger 1975; Salas & Kuruvila 1989; Lopez 1990, 1994; Beran & Culick 1992; Beran 1994). The numerical simulations based on the three-dimensional Navier–Stokes equations of Spall *et al.* (1990), Spall & Gatski (1991), and Breuer (1991) show certain situations where a nearly axisymmetric bubble may develop in the swirling flow. As was mentioned by Hall (1972) and Berger & Erlebacher (1995), although the various axisymmetric theories and simulations postulated different physical mechanisms of the vortex breakdown, they all lead to similar criteria for breakdown that shows agreement with the experiments. For example, the numerical simulations of Lopez (1990) of the axisymmetric case show good agreement with the flow visualization of Escudier (1984).

Therefore, the axisymmetric framework may serve as a reasonable base frame for the analysis of the nearly axisymmetric vortex breakdown phenomenon. This frame may give us insight into the mechanisms leading to the creation of the bubble, into the conditions for its appearance and into the flow structure ahead of it and around its nose. It is clear that for a complete understanding of the phenomenon we will also have to study in the future the stability of the axisymmetric bubble to non-axisymmetric perturbations and find the conditions for the bifurcation of asymmetric waves as well as the interaction of those waves in the wake of the bubble with the bubble.

As for the viscous effects on the process of vortex breakdown, we can see from the experiments that the nearly axisymmetric bubble develops under certain conditions at about one diameter of the pipe from the inlet. The characteristic time for a particle near

the centreline to travel from the inlet to the bubble nose is $t = D/U$ (D is the pipe diameter and U is the averaged axial speed along the centreline). On the other hand the diffusion time over this distance is $t_d = D^2/\nu$, and for water and air where ν, the viscosity, is small (where the Reynolds number is above 100) it is found that $t \ll t_d$ so that to the leading-order diffusion effects are small and the flow decelerating to stagnation and expanding around the bubble nose may be considered as inviscid. We recognize, however, that viscous effects become more important on the rear end of the bubble, within the bubble and in its wake, and may create some unsteadiness and determine the bubble nose position, but the bubble nose shape and the flow ahead of it are only slightly affected by the small viscosity. In fact, Bruecker (1995) and Bruecker & Althaus (1995) indicate that the axisymmetric and inviscid positive feedback mechanism proposed by Brown & Lopez (1992) reflects the experimental evidence of the development of a free stagnation point in the swirling flow and the nearly axisymmetric bubble behind it. Also, the criterion developed by Spall *et al.* (1987) shows no dependence on the Reynolds number (Re) for laminar swirling flows when $Re > 100$.

Finally, the results of Faler & Leibovich (1978), Uchida *et al.* (1985) and Bruecker & Althaus (1995) also show that the bubble shape is parabolic near the bubble nose. In fact, Bruecker & Althaus (1995) conducted a special experiment on swirling flow around a hollow hemispherical cap and claimed a strong resemblance of this flow with that around the bubble. The nose of the cap is parabolically expanding and behaves similarly to the bubble nose. The present results confirm this point.

This paper presents a theoretical analysis of the structure of an axisymmetric and inviscid swirling flow in the region around a vortex breakdown point. The model assumes that a free axisymmetric bubble surface is developed in the flow with a stagnation point at its nose. The flow development is studied in three regions: the approaching flow ahead of the bubble; around the bubble nose; and around the separated bubble surface (see §2). Asymptotic expansions are constructed in §3 to describe the flow ahead of and behind the stagnation point in terms of the radial distance from the vortex axis and from the bubble surface respectively. In the intermediate region around the stagnation point (§4), the flow is approximated by an asymptotic series of similarity terms that match the expansions in the other regions. As a result of this structure of solution the flow around the bubble nose can be analysed with no need to specify the flow inside the bubble. The analysis in §4 results in two possible matching processes and analytical expressions are given for the leading similarity term of the intermediate expansion in each of these processes. The first solution describes a swirling flow around a constant-pressure bubble surface, over which the flow is stagnant. The second solution represents a swirling flow around a pressure-varying bubble surface, where the flow expands along the bubble nose. In both solutions, the bubble nose has a parabolic shape and both exist only when $H' > 0$ (where H' is the derivative at the vortex centre of the total head H with the stream function ψ, and can be determined from the inlet flow conditions). This result is shown to be equivalent to Brown & Lopez's (1990) criterion for vortex breakdown. A general non-similarity solution near the bubble nose is given in §5, where the similarity solutions are special cases of this solution. Good agreement is found in the region around the stagnation point between the pressure-varying bubble solution and available experimental data of Faler & Leibovich (1978) and Uchida *et al.* (1985) for axisymmetric vortex breakdown (see §6).

It should be clarified that the criterion presented here depends upon the existence of the similarity solution and so lacks generality. However, since the axisymmetric

breakdown is dominated by the bubble shape (as is shown in the experiments of Bruecker & Althaus 1995), it is expected that the local flow near the bubble nose has a certain distinguished symmetry. The comparison in §6 shows that one of the special similarity solutions agrees nicely with the experimental data and that the structure of the flow near the bubble nose probably has the expected symmetry.

2. Basic problem and equations

An incompressible and inviscid steady axisymmetric swirling flow is considered in an (x, r)-space. The flow is described by the Euler equations;

$$\left.\begin{aligned} &w_x + u_r + u/r = 0, \\ &uu_r + wu_x - v^2/r = -p_r/\rho, \\ &uv_r + wv_x + uv/r = 0, \\ &uw_r + ww_x = -p_x/\rho. \end{aligned}\right\} \tag{1}$$

Here u, v, w are the radial, circumferential, and axial components of the velocity vector, and p and ρ = constant are the pressure and density of the flow, respectively. Using the definition of a stream function ψ, where

$$w = \frac{1}{r}\psi_r, \quad u = -\frac{1}{r}\psi_x, \tag{2a}$$

it can be shown (Batchelor 1967) that

$$rv = K(\psi), \quad p/\rho + \tfrac{1}{2}(u^2 + v^2 + w^2) = H(\psi). \tag{2b}$$

Here, K and H are the circulation and total head functions. The stream function $\psi(x, r)$ is determined by the Squire–Long equation (Squire 1956 and Long 1953 (also known as Bragg–Hawthorne 1950 equation)):

$$\psi_{xx} + \psi_{rr} - \frac{1}{r}\psi_r = r^2 H'(\psi) - I'(\psi), \tag{2c}$$

where $I = \frac{1}{2}K^2$. Also, $\psi(x, 0) = 0$ for every x.

We assume that a free axisymmetric bubble surface described by the equation $r = r_b(x)$ with $r_b(0) = 0$, is developed in the swirling flow, with a stagnation point at its nose, $x = 0$ (see figure 1). The separated bubble surface is also described by a $\psi(x, r = r_b(x)) = 0$ surface, where the bubble radius $r_b(x)$ needs to be solved. We have here a free boundary problem and we are specifically interested in describing the flow around the bubble surface where $\psi \geqslant 0$ as well as the local behaviour of $\psi(x, r)$ and $r_b(x)$ near $x = 0$.

Owing to the complicated geometry in the (x, r)-space, the present analysis also uses the transformation of variables $\psi(x, r)$ to $y \equiv r^2/2 = y(x, \psi)$. In the (x, ψ)-plane, the centreline ahead of $x = 0$ and the bubble surface for $x \geqslant 0$ occur along the $\psi = 0$ axis (see figure 2). The flow around the bubble is described in the $\psi \geqslant 0$ plane. Using a standard transformation analysis it can be shown from (2) that the function $y(x, \psi)$ is related to the velocity components by

$$w = \frac{1}{y_\psi}, \quad u = \frac{y_x}{(2y)^{1/2} y_\psi} \tag{3a}$$

and may be described by the equation (see also Keller & Egli 1985):

$$y_{\psi\psi}(y + \tfrac{1}{2}y_x^2) + \tfrac{1}{2}y_{xx}y_\psi^2 - y_x y_\psi y_{x\psi} + yy_\psi^3 H'(\psi) - \tfrac{1}{2}y_\psi^3 I'(\psi) = 0. \tag{3b}$$

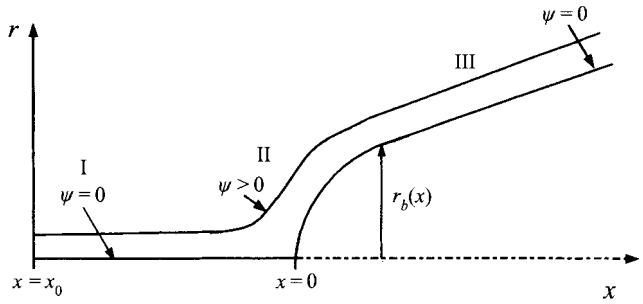

FIGURE 1. Axisymmetric vortex breakdown problem.

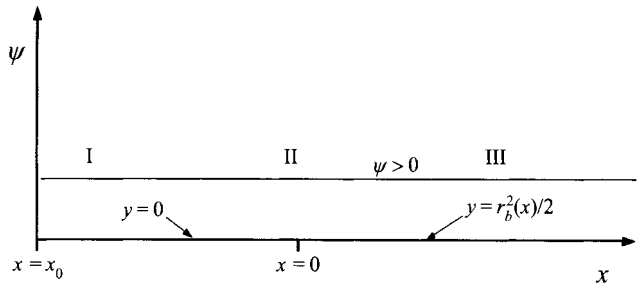

FIGURE 2. Problem formulation in the (x, ψ)-plane.

As is shown later, this transformation helps us to solve the flow around the bubble nose where $\psi \geqslant 0$ without any need to specify or analyse the nature of the flow inside the bubble (where $\psi < 0$).

In order to study the swirling flow around the bubble nose where $\psi \geqslant 0$, the flow field is approximated by asymptotic expansions in the limit $\psi \to 0^+$ in three regions: I the approaching flow ahead of the bubble; II around the bubble nose; and III around the bubble surface (see figures 1 and 2). In regions I and III, the coordinate x is fixed as $\psi \to 0^+$ (see §3). In the intermediate region II, a similarity solution that matches the expansions in the other regions is sought (§4). There, $\xi = x/\psi^k$ is fixed as $\psi \to 0^+$ (the similarity power k is to be determined). In §5, we discuss another possible non-similarity solution around the stagnation point that is based on the specific assumption of analytical continuation of the functions $H(\psi)$ and $K(\psi)$ inside the bubble, where $\psi < 0$. In §6, we compare the various solutions found to available experimental data on the axisymmetric vortex breakdown.

3. Analysis of regions I and III

3.1. *Approaching flow*

In the approaching flow region ahead of the bubble ($x < 0$), the asymptotic expansions of the velocity components and pressure may be given in the limit $r \to 0$ with x fixed in the form

$$\left.\begin{aligned} u &= a_0(x)\, r + a_3(x)\, r^3 + \ldots, \\ v &= b_0(x)\, r + b_3(x)\, r^3 + \ldots, \\ w &= c_0(x) + c_2(x)\, r^2 + \ldots, \\ p/\rho &= p_0(x) + p_2(x)\, r^2 + \ldots. \end{aligned}\right\} \tag{4}$$

The expansions omit a linear term in r in w and p and a quadratic term in r in u and v owing to viscous considerations or regularity conditions along the x-axis. Since $x = 0$ is the breakdown (stagnation) point, we have $c_0(0) = 0$.

It is also assumed that at an inlet station $x_0 < 0$, the functions $c_0(x_0), c_2(x_0), b_0(x_0)$, and $p_0(x_0)$ are given. From the basic system of equations (1), a sequence of relations is found:

$$\left.\begin{aligned} &a_0(x) = -\tfrac{1}{2}c_0'(x), \\ &b_0(x) = k_0\, c_0(x), \quad k_0 = b_0(x_0)/c_0(x_0), \\ &p_0(x)+\tfrac{1}{2}c_0^2(x) = p_0(x_0)+\tfrac{1}{2}c_0^2(x_0) \equiv p_{sto}/\rho, \\ &\tfrac{1}{2}c_0''(x)+2k_0^2\, c_0(x)+2c_2(x) = \text{constant} = H'. \end{aligned}\right\} \tag{5}$$

It is seen that the functions $a_0(x)$, $b_0(x)$ and $p_0(x)$ and can be determined by the three constant parameters k_0, p_{sto}, and H' and the change of the axial velocity $c_0(x)$ along the x-axis. It is also interesting to see that the ratio of the angular velocity $b_0(x)$ to the axial velocity $c_0(x)$ is kept constant along the centreline. As $x \to 0^-$, since $c_0(x) \to 0$, we also find that $b_0(x) \to 0$, which indicates the deviation of the swirl from solid-body rotation as the stagnation point is approached.

From (2a) and (4), we get as $r \to 0$

$$\psi(x, r) = \tfrac{1}{2}c_0(x)\, r^2 + \tfrac{1}{4}c_2(x)\, r^4 + \ldots, \tag{6}$$

so that as $\psi \to 0^+$, we find

$$y(x, r) \equiv \tfrac{1}{2}r^2 = \frac{\psi}{c_0(x)} - \frac{c_2(x)}{c_0^3(x)}\psi^2 + \ldots. \tag{7}$$

Therefore, as $\psi \to 0^+$:

$$K(\psi) \equiv rv = 2k_0\, \psi + \ldots, \tag{8a}$$

$$H(\psi) = p_{sto}/\rho + H'\psi + \ldots. \tag{8b}$$

From (5), the value of H' can be determined in terms of the given state of the flow at the centreline at station $x = x_0 < 0$ ahead of the stagnation point:

$$H' = \tfrac{1}{2}c_0''(x_0) + 2\frac{b_0^2(x_0)}{c_0(x_0)} + 2c_2(x_0). \tag{9}$$

Equation (9) shows that H' depends on the axial velocity at the centre at $x = x_0$, $c_0(x_0)$; the curvature of the jet/wake-like shape of the axial velocity near the centre, $c_2(x_0)$; the angular speed of the swirling flow, $b_0(x_0)$; and also on the second derivative of the axial velocity along the centreline, $c_0''(x_0)$. It can also be shown from (4) that the vorticity components (σ, η, ζ) in the radial, circumferential and axial directions, respectively, are given as $r \to 0$ by

$$\left.\begin{aligned} &\sigma \equiv -v_x = -b_0'(x)\, r + \ldots, \\ &\eta \equiv u_x - w_r = -r\,(\tfrac{1}{2}c_0''(x) + 2c_2(x)) + \ldots = r\left(2\frac{b_0^2(x_0)}{c_0^2(x_0)}\, c_0(x) - H'\right) + \ldots, \\ &\zeta \equiv (rv)_r/r = 2b_0(x) + \ldots. \end{aligned}\right\} \tag{10}$$

Therefore, H' may also be given by

$$H' = -\left(\frac{\eta}{r}\right)_{x_0} + 2\frac{b_0^2(x_0)}{c_0(x_0)} = -\left(\frac{\eta}{r}\right)_{x_0} + (\zeta)_{x_0}\frac{b_0(x_0)}{c_0(x_0)}. \tag{11}$$

H' may be determined by the vorticity components at the centre at $x_0 < 0$, as well as the axial and angular velocities at x_0. It is also interesting to see that as $x \to 0^-$, $c_0(x) \to 0$, and $\eta = -rH' + \ldots$, i.e. the azimuthal vorticity is negative near the stagnation point, $x = 0$, only when $H' > 0$.

3.2. *Flow around the separated bubble*

In the third region ($x > 0$) around the separated bubble surface $r = r_b(x)$, the asymptotic expansion for the function $y(x, \psi)$ may be given in the limit $\psi \to 0^+$ (or $r \to r_b(x)$) with x fixed by the general form

$$y(x, \psi) = d_0(x) + d_1(x)\,\psi^{\alpha} + d_2(x)\,\psi^{\beta} + \ldots, \tag{12}$$

where $0 < \alpha < \beta$ and $d_0(x) = r_b^2(x)/2 > 0$, and $r_b(x)$ is as yet unknown. Then, $y_\psi = d_1(x)\,\alpha\psi^{\alpha-1} + \ldots$. When $0 < \alpha < 1$, $y_\psi \to \infty$ as $\psi \to 0^+$ so the velocity components u and w vanish on the bubble surface. When $\alpha = 1$, u and w become

$$u = d_0'(x)/[(2d_0(x))^{1/2}\,d_1(x)] \quad \text{and} \quad w = 1/d_1(x)$$

along the bubble surface. When $\alpha > 1$ both u and w tend to infinity as $\psi \to 0^+$ which results in a non-physical situation. Therefore, α must satisfy $0 < \alpha \leqslant 1$.

The substitution of (8) and (12) into (3*b*) results in several cases relating the leading powers of ψ:

(i) When $0 < \alpha < 1/2$ or $1/2 < \alpha < 1$, we find that either $d_1(x) \equiv 0$ or $d_0(x) \equiv 0$. Both situations contradict the existence of a separated bubble at $x = 0$ and a flow developing around it.

(ii) $\alpha = 1/2$. Then both u and w vanish as $\psi \to 0^+$ (or $r \to r_b(x)$) and the bubble surface in this case is a stagnation surface along which the pressure is constant and equals p_{sto}. The functions $d_0(x)$ and $d_1(x)$ are related in the case $\alpha = 1/2$ by

$$d_0(x) + \tfrac{1}{2}(d_0'(x))^2 - \tfrac{1}{2}d_0(x)\,d_1^2(x)\,H' = 0. \tag{13a}$$

(iii) $\alpha = 1$ and $\beta = 2$. In this case, u and w change along the bubble surface as functions of x, as described above, and, therefore, the pressure also varies along the bubble surface. Here, functions $d_0(x)$, $d_1(x)$ and $d_2(x)$ are related by

$$2d_2(x)\,(d_0(x) + \tfrac{1}{2}(d_0'(x))^2) + \tfrac{1}{2}d_1^2(x)\,d_0''(x) - d_1(x)\,d_1'(x)\,d_0'(x) + H'd_0(x)\,d_1^3(x) = 0. \tag{13b}$$

We find that the general asymptotic expansion (12) constitutes only two possible consistent boundary conditions along the ($\psi = 0$, $x > 0$)-axis for solving equation (3*b*). One boundary condition may describe a separated stagnation surface (when $\alpha = 1/2$) and the other may describe a separated pressure-varying surface (when $\alpha = 1$). In this way the local problem for solving $y(x, \psi)$ around $x = 0$ and $\psi \geqslant 0$, that consists of (3*b*), (7) and (12) (with either $\alpha = 1/2$ or 1), is well-defined and there is no need to specify or analyse the nature of the flow inside the bubble for studying the flow around the bubble. We look now for local solutions around the stagnation point $x = 0$.

4. Flow around the stagnation point – similarity solution

In the intermediate region II, around the bubble nose ($x \sim 0$), the asymptotic expansion for the function y may be given in the limit $\psi \to 0^+$ and $x \to 0$ with $\xi = x/\psi^k$ fixed in the form

$$y = \psi^m f(\xi) + \ldots, \tag{14}$$

where k and m are similitude exponents ($k > 0$, $m > 0$) and $f > 0$ is the similarity

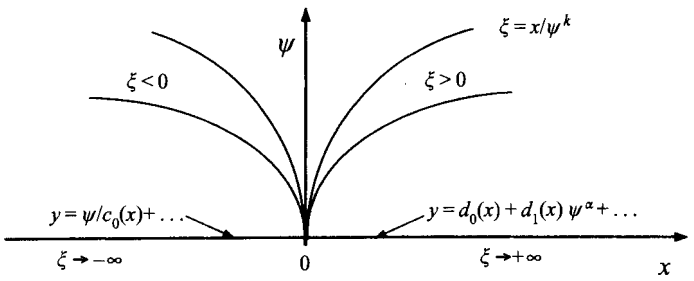

FIGURE 3. Similarity lines in the (x, ψ)-plane.

function. Expansion (14) must match the leading terms of the expansion (7) of the approaching flow as $\xi \to -\infty$ ($x < 0$, $\psi \to 0^+$), and those of the expansion (12) of the flow around the bubble as $\xi \to +\infty$ ($x > 0$, $\psi \to 0^+$) (see figure 3).

The substitution of (14) into (3*b*) and the use of (8) results in the following equation:

$$\psi^{2m-2}A + \psi^{3m-2k-2}B + \psi^{4m-3}H'C - \psi^{3m-2}k_0^2 D + \ldots = 0. \tag{15}$$

Here the terms A, B, C and D consist of complicated combinations of f, f_ξ, $f_{\xi\xi}$. As $\psi \to 0^+$, the last term in (15) is always smaller than the other terms and therefore is neglected. This means that the extended circulation function $I(\psi)$ may be neglected near the stagnation point. Equation (15) suggests six possible matching processes relating the leading powers of ψ:

$$\begin{aligned}
&(a)\ m = 1/2, && k = 1/4 && \text{where } A + B + H'C = 0,\\
&(b)\ m = 1/2, && k < 1/4 && \text{where } A + H'C = 0,\\
&(c)\ m = 1/2, && k > 1/4 && \text{where } B = 0,\\
&(d)\ m = 2k, && k < 1/4 && \text{where } C = 0,\\
&(e)\ m = 2k, && k > 1/4 && \text{where } A + B = 0,\\
&(f)\ m = 1 - 2k, && k \neq 1/4 && \text{where } B + H'C = 0.
\end{aligned}$$

Each of these equations is a complicated nonlinear ordinary differential equation for the solution of $f(\xi)$, and we now study each in turn.

4.1. (*a*) $m = 1/2$, $k = 1/4$

This may be the richest case. Here the function $f(\xi)$ is described by the equation

$$(f^2 + \tfrac{1}{2}\xi^2 f) f_{\xi\xi} + \tfrac{1}{2}\xi f_\xi f - 2f^2 - 2(f_\xi)^2 (f - \tfrac{3}{8}\xi f_\xi) + H' f (f - \tfrac{1}{2}\xi f_\xi)^3 = 0. \tag{16}$$

The approximation of f as $\xi \to -\infty$ by the asymptotic series

$$f \sim \bar{b}_a (-\xi)^{\bar{a}} + \bar{b}_{a1} (-\xi)^{\bar{a}_1} + \ldots \quad (\bar{a} > \bar{a}_1) \tag{17}$$

results from (14) for $x < 0$ and $\psi \to 0^+$ in

$$y = \psi^{1/2 - \bar{a}/4} \bar{b}_a (-x)^{\bar{a}} + \psi^{1/2 - \bar{a}_1/4} \bar{b}_{a1} (-x)^{\bar{a}_1} + \ldots . \tag{18}$$

Matching expansion (18) with (7) gives $\bar{a} = -2$ and $\bar{a}_1 = -6$. So,

$$f \sim \bar{b}_a (-\xi)^{-2} + \ldots \quad \text{as} \quad \xi \to -\infty. \tag{19}$$

The approximation of $f(\xi)$ as $\xi \to +\infty$ by the asymptotic series

$$f \sim b_a \xi^a + b_{a1} \xi^{a_1} + \ldots \quad (a > a_1) \tag{20}$$

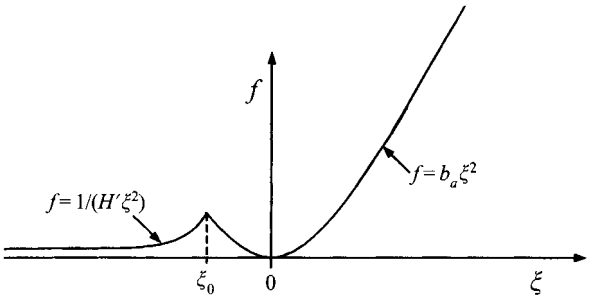

FIGURE 4. The similarity function $f(\xi)$ for the case $m = 1/2$, $k = 1/4$.

results from (14) for $x > 0$ and $\psi \to 0^+$ in

$$y = \psi^{1/2-a/4} b_a x^a + \dots . \tag{21}$$

Matching expansion (21) with (12) gives $a = 2$, $d_0(x) \sim b_a x^2 + \dots$ and

$$f \sim b_a \xi^2 + \dots \quad \text{as} \quad \xi \to +\infty. \tag{22}$$

The solution of (16) must therefore satisfy expansions (19) and (22).

On the other hand, it can be shown that both $f = 1/(H'\xi^2)$ and $f = b_a \xi^2$ are exact solutions of (16). Therefore, the continuous solution of (16) that also satisfies expansions (19) and (22) is given by (see figure 4)

$$f = \begin{cases} 1/(H'\xi^2) & \text{when} \quad \xi \leqslant \xi_0 \\ b_a \xi^2 & \text{when} \quad \xi \geqslant \xi_0, \end{cases} \tag{23}$$

where $\xi_0 = -(b_a H')^{-1/4}$. However, this solution does not describe a continuous physical flow around the separated bubble.

4.2. (*b*) $m = 1/2$, $k < 1/4$

In this case, the function $f(\xi)$ is described by the equation

$$-\tfrac{1}{4} f + k^2 \xi f_\xi + k^2 \xi^2 f_{\xi\xi} + H'(\tfrac{1}{2} f - k\xi f_\xi)^3 = 0. \tag{24}$$

Approximating f as $\xi \to -\infty$ by the asymptotic series (17) results, after matching (14) with (7), in $\bar{a} = -1/(2k)$ and $\bar{a}_1 = -3/(2k)$. So,

$$f \sim \bar{b}_a (-\xi)^{-1/(2k)} + \dots \quad \text{as} \quad \xi \to -\infty. \tag{25}$$

Approximating f as $\xi \to +\infty$ by the asymptotic series (20) results, after matching (14) with (12), in $a = 1/(2k)$ and $d_0(x) \sim b_a (x)^{1/(2k)} + \dots$. So,

$$f \sim b_a \xi^{1/(2k)} + \dots \quad \text{as} \quad \xi \to +\infty. \tag{26}$$

Solution of (24) must therefore satisfy expansions (25) and (26). Let

$$F \equiv \tfrac{1}{2} f - k\xi f_\xi, \tag{27}$$

then (24) takes the form

$$k\xi F' = H' F^3 - \tfrac{1}{2} F. \tag{28}$$

Equation (28) can be integrated to find

$$F = \pm [2(H' - C\xi^k)]^{-1/2}, \tag{29}$$

where C is constant. After integration, we get from (27)

$$f = b_a \xi^{1/(2k)} \pm \xi^{1/(2k)} \int_{-\infty}^{\xi} \frac{1}{k} \tilde{\xi}^{-(1+1/k)} [2(H' \tilde{\xi}^{1-2k+1/k} - C)]^{-1/2} \, \mathrm{d}\tilde{\xi}. \tag{30}$$

It is clear that solution (30) satisfies (25) if and only if $b_a = 0$ but this means that no bubble is separated at $x = 0$, in contrast to the basic assumptions of the analysis.

4.3. (*c*) $m = 1/2$, $k > 1/4$

In this case, the function $f(\xi)$ is described by the equation

$$f^2 f_{\xi\xi} - (f_\xi)^2((3-4k)f - 4k(1-k)\xi f_\xi) = 0. \tag{31}$$

An analysis similar to that described for cases (*a*) and (*b*) shows that solution of (31) must satisfy expansions (25) and (26) to match the similarity solution (14) with expansions (7) and (12) as $\xi \to -\infty$ and $\xi \to +\infty$, respectively. The substitution of (25) in (31) gives to the leading order, $O(\xi^{-2-3/(2k)})$, a linear equation for solving k, $2k-1 = 0$. Therefore, a solution of (31) that satisfies (25) can be found only when $k = 1/2 = m$. For $k = 1/2$, (31) takes the form

$$f^2 f_{\xi\xi} - (f_\xi)^2(f - \xi f_\xi) = 0. \tag{32}$$

It can be seen that solution of (32) can be given by $f = C_1 \bar{f}(\xi)$, with $\bar{f}(0) = 1$. Let $s \equiv \bar{f}$ and $t \equiv \xi \bar{f}_\xi$ be the phase-plane variables. Equation (32) is equivalent to the system

$$\frac{\mathrm{d}t}{\mathrm{d}s} - 1 = \frac{t(s-t)}{s^2}, \quad \frac{\mathrm{d}\xi}{\xi} = \frac{\mathrm{d}s}{t}. \tag{33a, b}$$

From (25), as $\xi \to -\infty$, we find that $s \to 0^+$ and $t = -s + \ldots$. From (26), as $\xi \to +\infty$, we find that $s \to \infty$ and $t = s + \ldots$. Also, as $\xi \to 0$, we find that $s = \bar{f}(0) = 1$ and $t = 0$ (provided that $\bar{f}_\xi(0)$ does not tend to infinity). It can be verified that the exact solution of (33*a*) that satisfies these three conditions is (see figure 5*a*)

$$t(s) = \frac{s^3 - s}{s^2 + 1}. \tag{34}$$

The substitution of (34) in (33*b*) gives after integration

$$C\xi = \frac{s^2 - 1}{s}, \tag{35}$$

where C is a constant of integration. Since $f > 0$ for every ξ, we get (see figure 5*b*)

$$f(\xi) = C_1 C \frac{\xi + (\xi^2 + 4/C^2)^{1/2}}{2}. \tag{36}$$

From (14) and (36), we find that as $\xi \to +\infty$ ($x > 0$, $\psi \to 0^+$)

$$y = \psi^{1/2} f\left(\frac{x}{\psi^{1/2}}\right) = C_1 C x + \psi\left(\frac{C_1}{Cx}\right) - \psi^2\left(\frac{C_1}{(Cx)^3}\right) + \ldots. \tag{37}$$

The matching of (37) and (12) shows that for the case $m = k = 1/2$ we have $\alpha = 1$, $\beta = 2$, $d_0(x) = C_1 C x$, $d_1(x) = C_1/Cx$, $d_2(x) = -C_1/(Cx)^3$. Therefore, (13*b*) should be satisfied. We find that $C_1 = (2/H')^{1/2}$, and solution exists only if $H' > 0$.

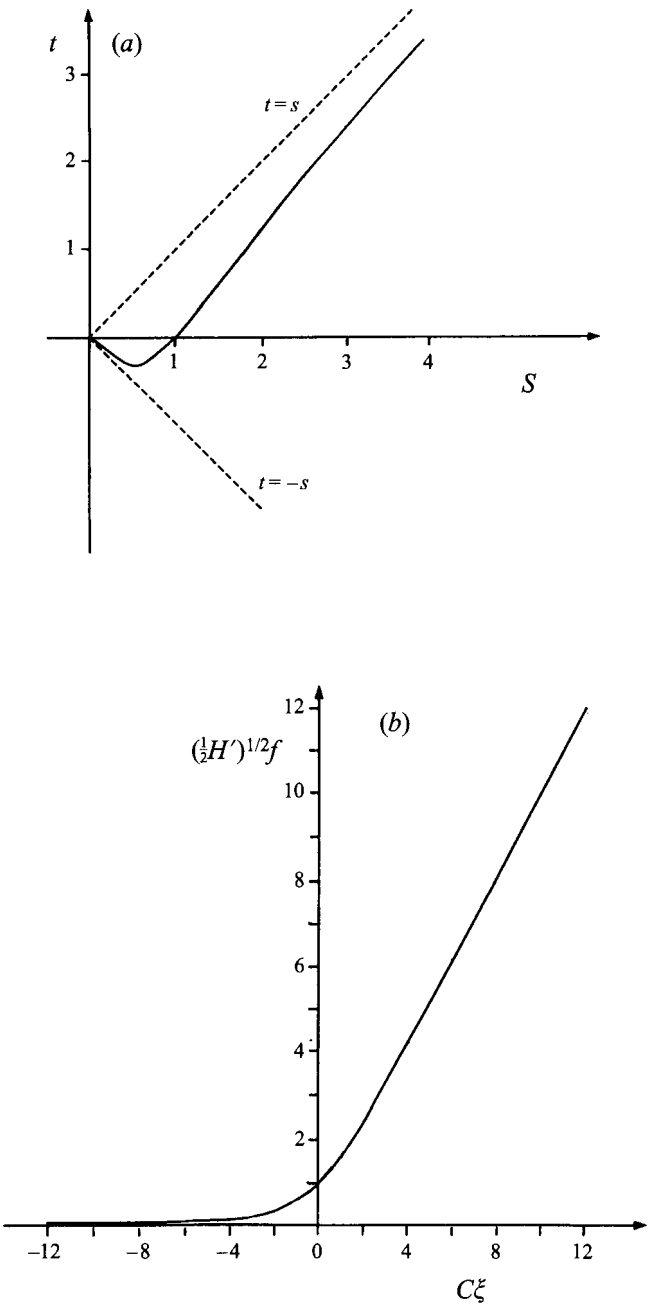

FIGURE 5. (*a*) The phase-plane solution $t(s)$ and (*b*) the similarity function $f(\xi)$, for the case $m = 1/2$, $k = 1/2$.

From (14) and (36) and with $\xi = x/\psi^{1/2}$, we find that as $x \to 0$ and $\psi \to 0^+$,

$$y = \tfrac{1}{2}(2/H')^{1/2} C[x + (x^2 + 4\psi/C^2)^{1/2}] + \ldots \tag{38}$$

or as $(x, y) \to 0$ and $\psi \geqslant 0$

$$\psi = \tfrac{1}{2}H' y(y - (2/H')^{1/2} Cx) + \ldots, \quad y = r^2/2. \tag{39}$$

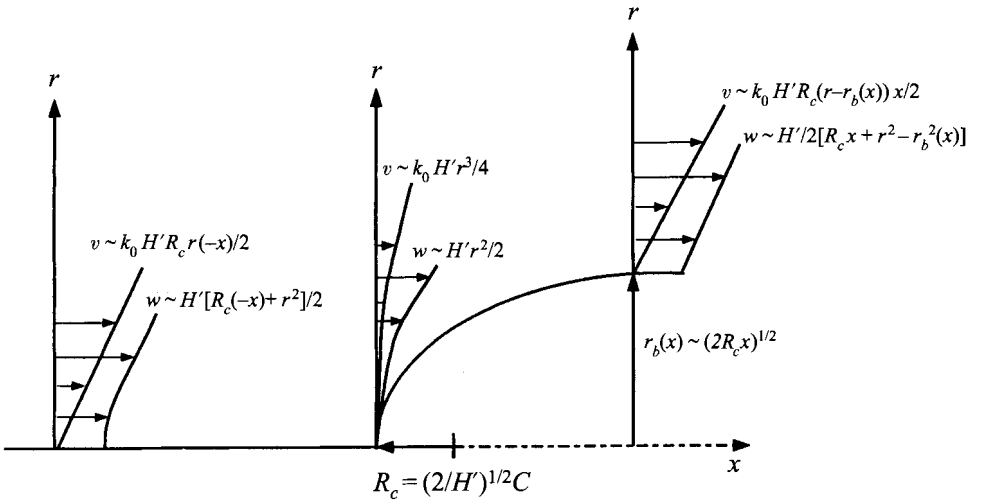

FIGURE 6. The flow around the nose of a pressure-varying bubble surface.

The local solution (39) shows that the bubble separated at $x = 0$ has the local shape of a paraboloid as $x \to 0^+$:

$$r_b(x) = [2(2/H')^{1/2} Cx]^{1/2} + \ldots \tag{40}$$

with a radius of curvature $R_c = (2/H')^{1/2} C$. The constant C represents a scale parameter related to the radius of curvature of the bubble nose and cannot be determined from the local analysis. This local solution describes a swirling flow around a pressure-varying bubble (see figure 6). As $x \to 0^-$,

$$w = (\tfrac{1}{2}H')^{1/2}\, C(-x) + \tfrac{1}{2}H' r^2 + \ldots, \quad v = (\tfrac{1}{2}H')^{1/2} k_0\, C(-x)\, r + \ldots. \tag{41}$$

The solution describes a wake-like deceleration of the axial velocity to stagnation which is a linear function of the distance from the stagnation point, and a decay of the solid-body rotation in the swirl component as the stagnation point is approached. At $x = 0$ (stagnation point station)

$$w = \tfrac{1}{2}H' r^2 + \ldots, \quad v = \tfrac{1}{4} k_0 H' r^3 + \ldots. \tag{42}$$

The axial velocity keeps its wake-like shape with a specific curvature $H'/2$, but the circumferential velocity changes from solid-body rotation to a much slower swirl that is changing as the cubic power of the radial distance from the centreline. Around the bubble surface $r = r_b(x)$ given by (40) the velocity components are

$$w = (\tfrac{1}{2}H')^{1/2}\, Cx + \tfrac{1}{2}H'(r^2 - r_b^2(x)) + \ldots, \quad v = 2(\tfrac{1}{2}H')^{1/2} k_0\, C(r - r_b(x))\, x + \ldots. \tag{43}$$

The axial flow accelerates (from stagnation) along the bubble paraboloid surface as a linear function of the distance from the stagnation point. Swirl vanishes on the bubble surface but increases linearly as the axial or radial distances from the bubble are increased.

4.4. (*d*) $m = 2k$, $k < 1/4$

In this case, the function $f(\xi)$ is described by the equation

$$2f - \xi f_\xi = 0. \tag{44}$$

The solution of (44) is given by $f = b_a \xi^2$ and then $y = x^2 + \ldots$. However this solution does not satisfy the expansion (7) for the approaching flow.

4.5. (*e*) $m = 2k$, $k > 1/4$

In this case, the function $f(\xi)$ is described by the equation

$$2k(f^2+\tfrac{1}{2}\xi^2 f)f_{\xi\xi}+(1-3k)\xi f f_\xi-2(1-2k)f^2-(f_\xi)^2\left(f-\frac{1-k}{2}\xi f_\xi\right)=0. \tag{45}$$

The approximation of $f(\xi)$ as $\xi\to-\infty$ by the asymptotic series (17) results, from matching with (7), in $\bar{a}=2-1/k$ and $\bar{a}_1=2-2/k$ and

$$f\sim \bar{b}_a(-\xi)^{2-1/k}+\bar{b}_{a1}(-\xi)^{2-2/k}+\dots \quad \text{as} \quad \xi\to-\infty. \tag{46}$$

The approximation of $f(\xi)$ as $\xi\to\infty$ by the asymptotic series (20) results from (14) in

$$y=\psi^{2k-ka}b_a x^a+\psi^{2k-ka_1}b_{a1}x^{a_1}+\dots. \tag{47a}$$

Matching expansion (47) with (12) gives $a=2$, $a_1=2-\alpha/k$ (where $\alpha=1/2$ or 1), $d_0(x)\sim b_a x^2+\dots$ and

$$f\sim b_a\xi^2+b_{a1}\xi^{a_1}+\dots \quad \text{as} \quad \xi\to\infty. \tag{47b}$$

When $\alpha=1/2$, we find $a_1=2-1/(2k)$. Substituting (47) into (45) results to the leading order, $O(\xi^{4-1/(2k)})$, in $b_a=0$ or $b_a=1/2$ or $b_{a1}=0$. All of these contradict the assumption of a separated bubble at $x=0$. Therefore we may only have $\alpha=1$ and then $a_1=2-1/k$ and

$$f\sim b_a\xi^2+b_{a1}\xi^{2-1/k}+\dots \quad \text{as} \quad \xi\to\infty. \tag{48}$$

We look for a solution of (45) that satisfies conditions (46) and (48). Let $s\equiv f/\xi^2$ and $t\equiv f_\xi/\xi$ be the phase-plane variables, then equation (45) is equivalent to the system

$$(t-2s)\frac{\mathrm{d}t}{\mathrm{d}s}+t=\frac{t^2(s-(1-k)t/2)+2(1-2k)s^2-(1-3k)ts}{2ks(s+\frac{1}{2})}, \quad \frac{\mathrm{d}\xi}{\xi}=\frac{\mathrm{d}s}{t-2s}. \tag{49}$$

From (46), as $\xi\to-\infty$, we find that $s\to0$ and $t=(2-1/k)s+\dots$. From (48), as $\xi\to+\infty$, we find that $s=b_a$ and $t=2b_a$. Also, as $\xi\to0\pm$, we find that $s\to\infty$ and $t=\pm Cs^{1/2}+\dots$. It may also be shown from (48) that as $\xi\to\infty$, $\mathrm{d}t/\mathrm{d}s=2-1/k$ and

$$t=2b_a+a_1(s-b_a)+\dots \quad \text{as} \quad s\to b_a. \tag{50}$$

The substitution of (50) into (49) results to the leading order, $O(s-b_a)$, in a special similarity power $k=1/2$ and so $m=1$ and $\bar{a}=a_1=0$. This gives that as $\xi\to-\infty$, $f\sim b_a+O((-\xi)^{-2})$ and from (7) and (14) we get $c_0(x)=1/b_a$ as $x\to0^-$ and $\psi\to0^+$. This means, however, that the axial velocity component is constant near $x=0$ and cannot reach stagnation at $x=0$ unless $b_a\to\infty$, which does not lead to a relevant solution in this case.

4.6. (*f*) $m=1-2k$, $k\neq1/4$

In this case, the function $f(\xi)$ is described by the equation

$$f^2f_{\xi\xi}-2(f_\xi)^2\left(f-\frac{k(1-k)}{2m^2}\xi f_\xi\right)+2mH'f\left(f-\frac{k}{m}\xi f_\xi\right)^3=0. \tag{51}$$

Approximating $f(\xi)$ as $\xi\to-\infty$ by the asymptotic series (17) results, after matching (14) with (7), in $\bar{a}=-2$ and $\bar{a}_1=-2-1/k$ and

$$f\sim \bar{b}_a(-\xi)^{-2}+\bar{b}_{a_1}(-\xi)^{-2-1/k}+\dots \quad \text{as} \quad \xi\to-\infty. \tag{52}$$

The substitution of (52) into (51) shows to the leading order, $O(\xi^{-8})$, that $\bar{b}_a=1/H'$.

Approximating $f(\xi)$ as $\xi \to +\infty$ by the asymptotic series (20) results, from matching (14) with (12), in $a = 1/k-2$ and

$$f \sim b_a \xi^{1/k-2} + \ldots \quad \text{as} \quad \xi \to +\infty. \tag{53}$$

We look for a solution of (51) that satisfies conditions (52) and (53). Let $s = \xi^2 f$ and $t = \xi^3 f_\xi$ be the phase-plane variables. Equation (51) is equivalent to the system

$$(t+2s)\frac{\mathrm{d}t}{\mathrm{d}s} - 3t = \frac{1}{s^2}\left(2t^2\left(s - \frac{k(1-k)}{2m^2}t\right) - 2mH's\left(s - \frac{k}{m}t\right)^3\right), \quad \frac{\mathrm{d}\xi}{\xi} = \frac{\mathrm{d}s}{t+2s}. \tag{54}$$

From (52), as $\xi \to -\infty$, we find that $s = 1/H'$ and $t = -2/H'$. From (53) as $\xi \to +\infty$, we find that $s \to +\infty$ and $t = (m/k)s + \ldots$. Also, as $\xi \to 0\pm$, we find that $t = \pm Cs^{3/2} + \ldots$. It may also be shown from (52) that as $\xi \to -\infty$, $\mathrm{d}t/\mathrm{d}s = \bar{a}_1 = -2 - 1/k$ and

$$t = -2/H' - (2+1/k)(s - 1/H') + \ldots \quad \text{as} \quad s \to (1/H')^-. \tag{55}$$

The substitution of (55) into (54) results to the leading order, $O(s-1/H')$, in a specific equation for solving k:

$$12k^2 - 7k + 1 = 0. \tag{56}$$

The solution of (56) gives $k = 1/4$ which is excluded in this case, and $k = 1/3$ for which $m = 1/3$ and

$$y = \psi^{1/3} f(\xi) + \ldots, \quad \xi = x/\psi^{1/3}. \tag{57}$$

Here $f(\xi)$ is described by the equation (using (51))

$$f^2 f_{\xi\xi} - 2f_\xi^2(f - \xi f_\xi) + \tfrac{2}{3}H' f(f - \xi f_\xi)^3 = 0 \tag{58}$$

or by the equivalent system (using (54))

$$(t+2s)\frac{\mathrm{d}t}{\mathrm{d}s} - 3t = [2t^2(s-t) - 2/3H's(s-t)^3]/s^2, \quad \frac{\mathrm{d}\xi}{\xi} = \frac{\mathrm{d}s}{t+2s}, \tag{59a, b}$$

with the following conditions:

$$\left.\begin{aligned} &t = -2/H' - 5(s - 1/H') + \ldots \quad \text{as} \quad s \to (1/H')^-, \\ &t = s + \ldots \quad \text{as} \quad s \to +\infty, \\ &t = \pm C s^{3/2} + \ldots \quad \text{as} \quad s \to 0^\pm. \end{aligned}\right\} \tag{60}$$

It may be verified that the exact solution of (59*a*) which satisfies conditions (60) is given by two branches (see figure 7*a*)

$$\left.\begin{aligned} t &= \frac{H'^{1/2} s^{3/2}}{H'^{1/2} s^{1/2} - 3/2} \quad \text{when} \quad 0 \leqslant s \leqslant 1/H' \quad \text{for} \quad \xi < 0, \\ t &= \frac{H'^{1/2} s^{3/2}}{H'^{1/2} s^{1/2} + 3/2} \quad \text{when} \quad 0 \leqslant s < \infty \quad \text{for} \quad \xi > 0. \end{aligned}\right\} \tag{61}$$

The solution given by (61) exists only when $H' > 0$. Integration of (59*b*) gives

$$\left.\begin{aligned} \xi &= C^3 \frac{s^{3/2}}{H'^{1/2} s^{1/2} - 1} \quad \text{when} \quad 0 \leqslant s \leqslant 1/H' \quad \text{for} \quad \xi < 0, \\ \xi &= C^3 \frac{s^{3/2}}{H'^{1/2} s^{1/2} + 1} \quad \text{when} \quad 0 \leqslant s < \infty \quad \text{for} \quad \xi > 0, \end{aligned}\right\} \tag{62}$$

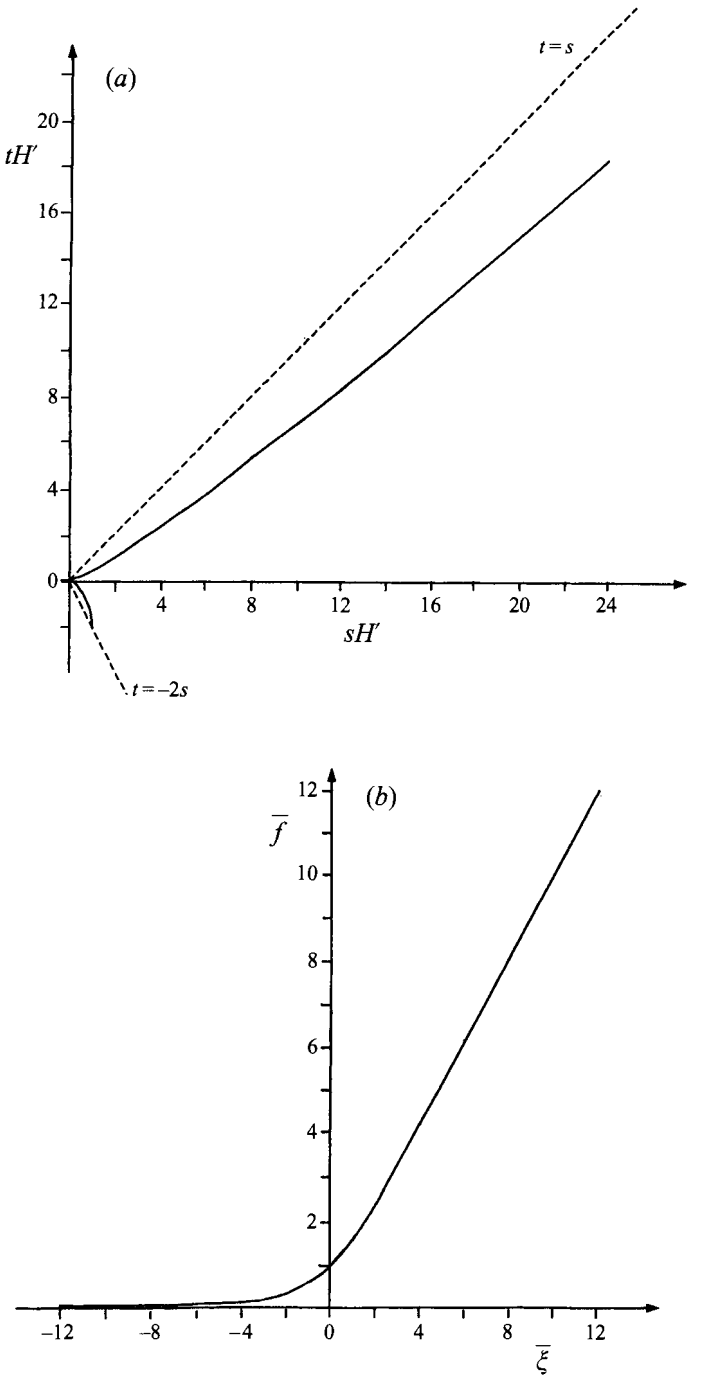

FIGURE 7. (*a*) The phase-plane solution $t(s)$ and (*b*) the similarity function $f(\xi)$, for the case $m = 1/3$, $k = 1/3$.

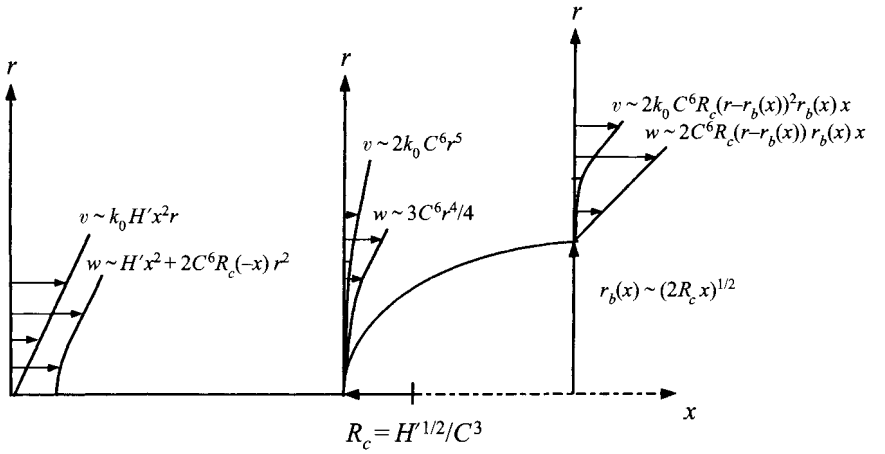

FIGURE 8. The flow around the nose of a stagnation bubble surface.

where C is a constant of integration. From the definitions of s and t and (62) the function $f(\xi)$ can be described by the parametric representation

$$\left.\begin{aligned} &f = \frac{1}{C^2}\bar{f}(\bar{\xi}), \quad \bar{\xi} = \frac{H'^{1/2}}{C}\xi, \\ &\bar{f} = \frac{\gamma}{(\gamma-1)^{1/3}}, \quad \bar{\xi} = (\gamma-1)^{2/3} \quad \text{when} \quad 0 \leqslant \gamma \leqslant 1 \quad \text{for} \quad \xi < 0, \\ &\bar{f} = \frac{\gamma}{(\gamma+1)^{1/3}}, \quad \bar{\xi} = (\gamma+1)^{2/3} \quad \text{when} \quad 0 \leqslant \gamma \leqslant \infty \quad \text{for} \quad \xi > 0. \end{aligned}\right\} \tag{63}$$

The function $\bar{f}(\bar{x})$ is described in figure 7(*b*). It is a monotonically increasing function that changes like $O((-\xi)^{-2})$ as $\xi \to -\infty$ and $O(\xi)$ as $\xi \to +\infty$. The function $\bar{f}(\bar{\xi})$ also satisfies the relation

$$\bar{f}^{3/2} - \bar{\xi}\bar{f}^{1/2} - 1 = 0. \tag{64}$$

From equations (57) and (63), it is found that as $\xi \to +\infty (\gamma \to +\infty$ or $x \to 0^+$ and $\psi \to 0^+)$

$$y = \psi^{1/3} f\left(\frac{x}{\psi^{1/3}}\right) = \frac{H'^{1/2}}{C^3}x + \frac{(H'^{1/2})^{-1/2}}{C^{3/2}}\frac{\psi^{1/2}}{x^{1/2}} + \ldots. \tag{65}$$

The matching of (65) and (12) shows that for the case $m = k = 1/3$ we have $\alpha = 1/2$, $d_0(x) = (H'^{1/2}/C^3)x$, $d_1(x) = (H'^{1/2})^{-1/2}/(C^{3/2}x^{1/2})$ and (13*a*) is automatically satisfied as $x \to 0^+$. From equations (57), (63) and (64), we can also resolve the local behaviour of ψ as both $(x, y) \to 0$ and $\psi \geqslant 0$:

$$\psi = C^6 y\left(y - \frac{H'^{1/2}}{C^3}x\right)^2 + \ldots, \quad y = r^2/2. \tag{66}$$

The local solution (66) shows that the bubble separated at $x = 0$ has the local shape of a paraboloid as $x \to 0^+$:

$$r_b(x) = [(2\sqrt{H'}/C^3)x]^{1/2} + \ldots \tag{67}$$

with a radius of curvature $R_c = H'^{1/2}/C^3$. The constant C^3 represents a scale parameter related to the radius of curvature of the bubble nose and cannot be determined from the local analysis. This local solution describes a swirling flow around a stagnation surface (see figure 8). As $x \to 0^-$

$$w = H'x^2 + 2C^3 H'^{1/2} r^2(-x) + \ldots, \quad v = k_0 H' x^2 r + \ldots . \tag{68}$$

The solution describes a wake-like deceleration of the axial velocity to stagnation that is a quadratic function of the distance from the stagnation point and with specific curvature H'. The solid-body rotation of the swirl component decays as the stagnation point is approached. At $x = 0$ (stagnation point station)

$$w = \tfrac{3}{4} C^6 r^4 + \ldots, \quad v = 2k_0 C^6 r^5 + \ldots . \tag{69}$$

The axial velocity changes its wake-like shape from quadratic in r to quartic in r. The circumferential velocity deviates strongly from solid-body rotation to a much slower swirl that is changing as the fifth power of the radial distance from the centreline. Around the bubble, $r = r_b(x)$ given by (67), the velocity components are

$$\left.\begin{aligned} w &= 2C^3 H'^{1/2}(r - r_b(x))\, r_b(x)\, x + \ldots, \\ v &= 2k_0 C^3 H'^{1/2}(r - r_b(x))^2 r_b(x)\, x + \ldots . \end{aligned}\right\} \tag{70}$$

The flow along the bubble surface is stagnant. The axial velocity increases linearly and the circumferential velocity increases quadratically as the radial distance from the bubble surface is increased.

4.7. *Summary of similarity solutions*

The six matching processes described above, §§4.1–4.6, of a similarity solution (14) with the asymptotic behaviour of the approaching flow (equation (7)) and with that of the flow around the separated bubble (equation (12)) results in two distinct local solutions to describe the nature of an axisymmetric swirling flow around a stagnation point. The first solution describes a swirling flow that expands around a pressure-varying bubble surface (see (38)–(43) and figure 6). The second solution describes a swirling flow around a stagnation surface ((63)–(70) and figure 8). In both solutions, the bubble nose has a paraboloid shape and they are given in terms of a constant scale parameter that is related with the local radius of curvature of the bubble nose. Also, both solutions exist only when $H' > 0$ or according to (9) when at some inlet station $x_0 < 0$ ahead of the stagnation point

$$\tfrac{1}{2} c_0''(x_0) + 2\frac{b_0^2(x_0)}{c_0(x_0)} + 2c_2(x_0) > 0. \tag{71}$$

The meaning of the condition $H' > 0$ is that the vortex flow is more receptive to breakdown when the stagnation pressure at the vortex centre is smaller than at its surroundings.

It is also easy to see from (11) that the necessary condition $H' > 0$ means that as $r \to 0$

$$\alpha_0 = \frac{v}{w}\bigg|_{x_0} = \frac{b_0(x_0)\, r + \ldots}{c_0(x_0) + \ldots} > \frac{\eta}{\zeta}\bigg|_{x_0} \equiv \beta_0, \tag{72}$$

which is exactly the Brown & Lopez (1990) criterion for the occurrence of vortex breakdown. It should be pointed out, however, that in this work, this criterion has been found directly from the analytical solutions for the similarity term (14). It is also interesting to note that for the two solutions, the azimuthal vorticity near the stagnation point is negative and given by

$$\eta(x = 0,\ r \to 0) = -rH' + \ldots < 0 \tag{73}$$

(see also (10)).

5. Flow around the stagnation point – a non-similarity solution

In the intermediate region, around the bubble nose $x \sim 0$, we may consider the assumption of an analytical continuation of the functions $H(\psi)$ and $I(\psi)$ for $\psi < 0$ inside the bubble (see (2)). Under this specific assumption, we may describe the local solution around $x = 0$ of (2*c*) by the asymptotic series (a non-similarity solution)

$$\psi(x,y) \sim A_1 x + B_1 y + A_2 x^2 + B_2 xy + C_2 y^2 + A_3 x^3 + B_3 x^2 y + C_3 xy^2 + D_3 y^3 + \ldots \quad \text{as} \quad (x,y) \to 0. \tag{74}$$

The requirement that $\psi_x(x,0) = 0$ for every x (no radial velocity along the centreline) results in $A_1 = A_2 = A_3 = \ldots 0$. The assumption that $\psi_y(0,0) = 0$, gives $B_1 = 0$. The substitution of (74) into (2*c*), together with (8*a*) and (8*b*), results as $(x,y) \to 0$ in a leading-order relation

$$2C_2 + B_3 = H'. \tag{75}$$

Let $C_2 = \frac{1}{2}\tau H'$ and $B_3 = (1-\tau)H'$. Then, as $(x,y) \to 0$, we find

$$\psi = \tfrac{1}{2}\tau H' y^2 + B_2 xy + (1-\tau) H' x^2 y + C_3 xy^2 + D_3 y^3 + \ldots . \tag{76}$$

In the general case, where $\tau \neq 0$ and $B_2 \neq 0$, the local flow around the stagnation point is described to the leading order by two parameters, $\tau H' = \partial w/\partial y|_{(0,0)}$ and $B_2 = \partial w/\partial x|_{(0,0)}$, that are related to the derivatives of the axial velocity w at the stagnation point ($x = y = 0$).

Assuming also a wake-like deceleration of the axial velocity ahead of the stagnation point, as $x \to 0^-$, we find from

$$w = \psi_y = \tau H' y + B_2 x + \ldots, \quad v = k_0 B_2 xr + \tau k_0 H' r^3/4 + \ldots \tag{77}$$

that $B_2 < 0$ and $\tau H' \geqslant 0$. Therefore, $(-B_2)/(\tau H') > 0$ and $\psi = 0$ along the $y = 0$ axis and along the separated bubble with a paraboloid nose

$$r = r_b(x) = 2\left(\frac{(-B_2)}{\tau H'}\right)^{1/2} x + \ldots . \tag{78}$$

At the stagnation point $x = 0$

$$w = \tfrac{1}{2}\tau H' r^2 + \ldots, \quad v = \tfrac{1}{4}\tau k_0 H' r^3 + \ldots . \tag{79}$$

Around the separated bubble $r = r_b(x)$,

$$w = (-B_2)\, x + \tau H'(r - r_b(x))\, r_b(x) + \ldots, \quad v = 2k_0(-B_2)\,(r - r_b(x))\, x + \ldots . \tag{80}$$

Equations (80) describe in the general case a swirling flow around a pressure-varying surface (78). However, as was indicated in the Introduction, it can be seen that inside the bubble where $0 < r < r_b(x)$ the analytical continuation assumption results in the solution (80) which predicts swirl velocities that are opposite to those outside the bubble. It seems that this result does not properly represent the physical observation inside the bubble (see the experiments of Faler & Leibovich 1978 and Uchida *et al.* 1985). It is also clear that when $\tau = 1$, asymptotic solution (76) becomes, for $\psi \geqslant 0$, the asymptotic solution (39) of a swirling flow around a pressure-varying surface with a paraboloid nose, where $(-B_2) = (H'/2)^{1/2} C$. On the other hand, when $\tau = 0$, $B_2 = 0$, $C_3 = -2H'^{1/2} C^3$ and $D_3 = C^6$ solution (76) becomes, for $\psi \geqslant 0$, the asymptotic solution (66) of a swirling flow around a stagnation bubble surface. As indicated in §3, solution (76) describes negative azimuthal vorticity η around the stagnation point only when $H' > 0$ and so a separation bubble exists only when $\tau \geqslant 0$.

6. Comparison with experimental data

The local solutions described above are compared in this section with the available detailed experimental data of Faler & Leibovich (1978) and Uchida *et al.* (1985) on axisymmetric vortex breakdown. In both cases, the data given for cross-sections ahead of breakdown and along the vortex centreline provide all the information needed to estimate the parameter k_0 and H' (given by (5) and (9)).

From the experimental data of Faler & Leibovich (1978), we can estimate at an upstream cross-section $x_0 = -14.6$ mm, ahead of the stagnation point, that $c_0(x_0) = (12.2 \pm 0.4)$ cm s^{-1}, $c_2(x_0) = (+20 \pm 10)$ cm^{-1} s^{-1}, $b_0(x_0) = (30 \pm 3)$ s^{-1} and $c_0''(x_0) = (-15 \pm 5)$ cm^{-1} s^{-1} (see figure 9). From these we find $k_0 = (2.4 \pm 0.3)$ cm^{-1}, $H' = (180 \pm 30)$ cm^{-1} s^{-1}. Similar estimations for k_0 and H' may be found at other cross-sections $x = -6.6$ mm, $x = -4.0$ mm and $x = -3.0$ mm ahead of the breakdown point (see Faler & Leibovich 1978). This demonstrates that both parameters k_0 and H' are constant and positive along the vortex centreline, as is predicted by the present axisymmetric and inviscid analysis. Of specific interest is comparing the wake-like shape of the flow at a cross-section $x = -1.0$ mm, just ahead of the stagnation point. We find that $c_2(x = -1.0 \text{ mm}) = (85 \pm 10)$ cm^{-1} s^{-1} (figure 9) which correlates nicely with $c_2 = H'/2 + \ldots$ predicted by (41) of the pressure-varying bubble solution or by the case $\tau \approx 1$ in (76)–(80). This solution also predicts a linear deceleration of the axial velocity along the centreline as a function of the axial distance x from the stagnation point (see (41)) as is also shown in figure 9 for the data taken from figure 6 of Faler & Leibovich (1978). The predictions of the other solution, describing a stagnation surface (see (68)) do not correlate with the behaviour shown in Faler & Leibovich (1978) (see figure 9).

Using the experimental data of Uchida *et al.* (1985, figures 8 and 12), we can estimate at an inlet cross-section $x_0 = -40$ mm, ahead of the stagnation point, that $c_0(x_0) = (2.5 \pm 0.1)\, W_m$, $c_2(x_0) = (-10 \pm 1)\, W_m/R^2$, $b_0(x_0) = (8.5 \pm 0.4)\, W_m/R$ and $c_0''(x_0) = (-6 \pm 2)\, W_m/R^2$ (see figure 10). Here W_m is a reference speed and R is the tube radius. From these we find $k_0 = (3.4 \pm 0.3)/R$ and $H' = (35 \pm 8)\, W_m/R^2$. Similar estimations for k_0 and H' may also be found at other cross-sections, $x = -20$ mm, $x = -10$ mm and $x = -4$ mm ahead of the breakdown point (see Uchida *et al.* 1985). Again, the experimental data demonstrate that both parameters k_0 and H' are constant and positive along the vortex centreline, as is predicted by the present analysis. It is also interesting to analyse the wake-like shape of the axial velocity at the stagnation point station $x = 0$. We find that $c_2(x = 0) = (16 \pm 2)\, W_m/R^2$ which correlates with $c_2 = H'/2$ predicted by (41) and (42) or with the case $\tau \approx 1$ in (76)–(80). It is also clear from the experimental data that the circumferential velocity deviates from solid-body rotation near the centre to a rotation that depends on r^3 as given by (42). The linear deceleration of the axial velocity near the stagnation point given by (41) seems to fit the experimental data of Uchida *et al.* (1985) better than that described by (68) (see figure 10). We may conclude that in the nose region of the axisymmetric breakdown, the pressure-varying bubble solution described by (39)–(43) shows good agreement with the experimental data of both Faler & Leibovich (1978) and Uchida *et al.* (1985).

The experimental data also show that, in general, at inlet cross-sections far ahead of the stagnation point, $c_0''(x_0)$ is small and may be neglected in the calculation of H' by (9). In such cases, the necessary condition (71) for the existence of the two similarity solutions takes the form

$$b_0(x_0) > [c_0(x_0)(-c_2(x_0))]^{1/2}. \tag{81}$$

There is a lower limit for the angular velocity at the inlet $x_0 < 0$ for a stagnation point

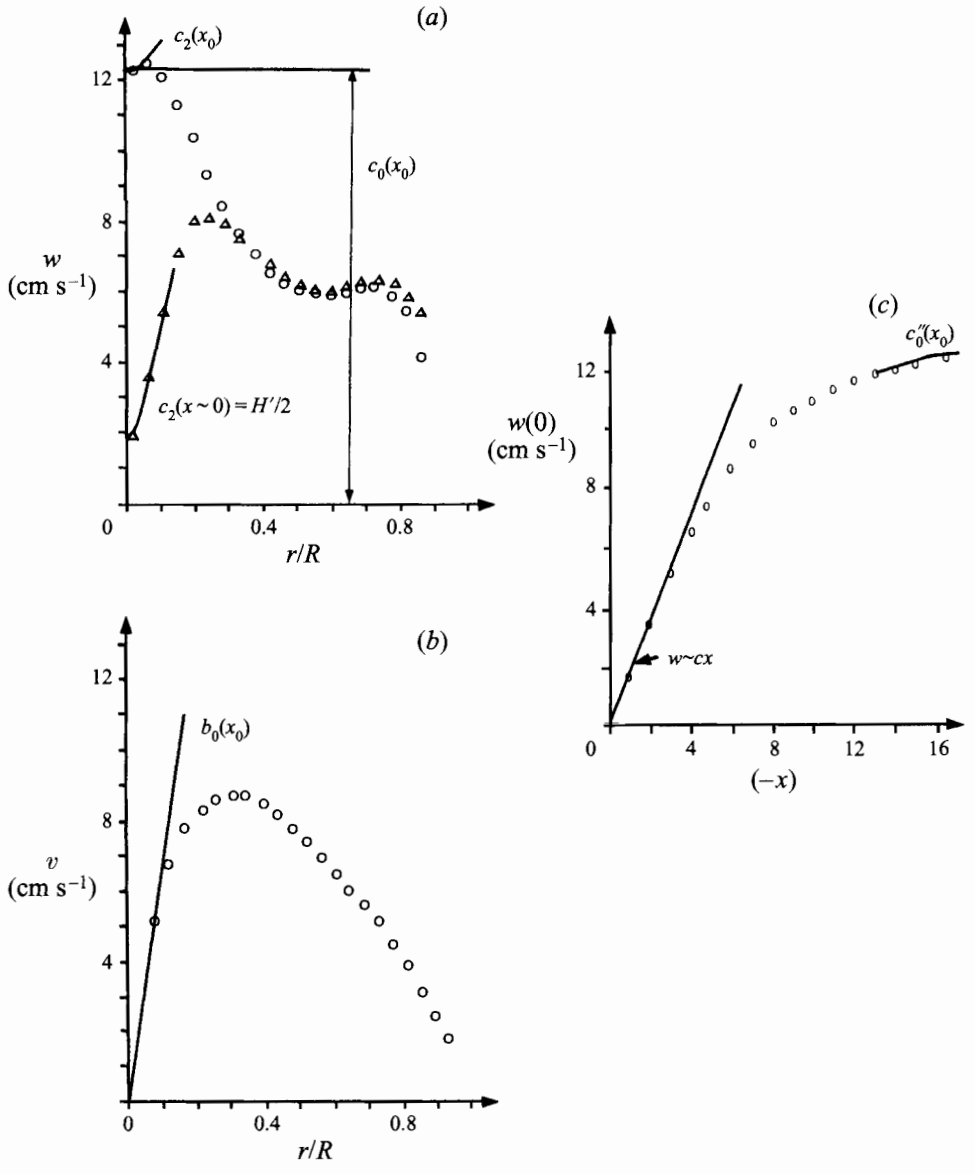

FIGURE 9. Comparison of the present solutions with the experimental data of Faler & Leibovich (1978).

to exist along the vortex centreline. In the case of an inlet flow described by the Q-vortex (Leibovich 1984)

$$w = W_0 + W_1 e^{-\beta r^2}, \quad v = K(1 - e^{-\beta r^2})/r \tag{82}$$

we find that $b_0(x_0) = K\beta$, $c_0(x_0) = W_0 + W_1$ and $-c_2(x_0) = \beta W_1$. With the definitions $q \equiv K\beta^{1/2}/W_1$ and $\delta \equiv W_1/W_0$ one concludes that axisymmetric vortex breakdown may exist only if

$$q > (1 + 1/\delta)^{1/2}. \tag{83}$$

A stagnation point cannot develop in a Q-vortex flow with relatively low swirl where

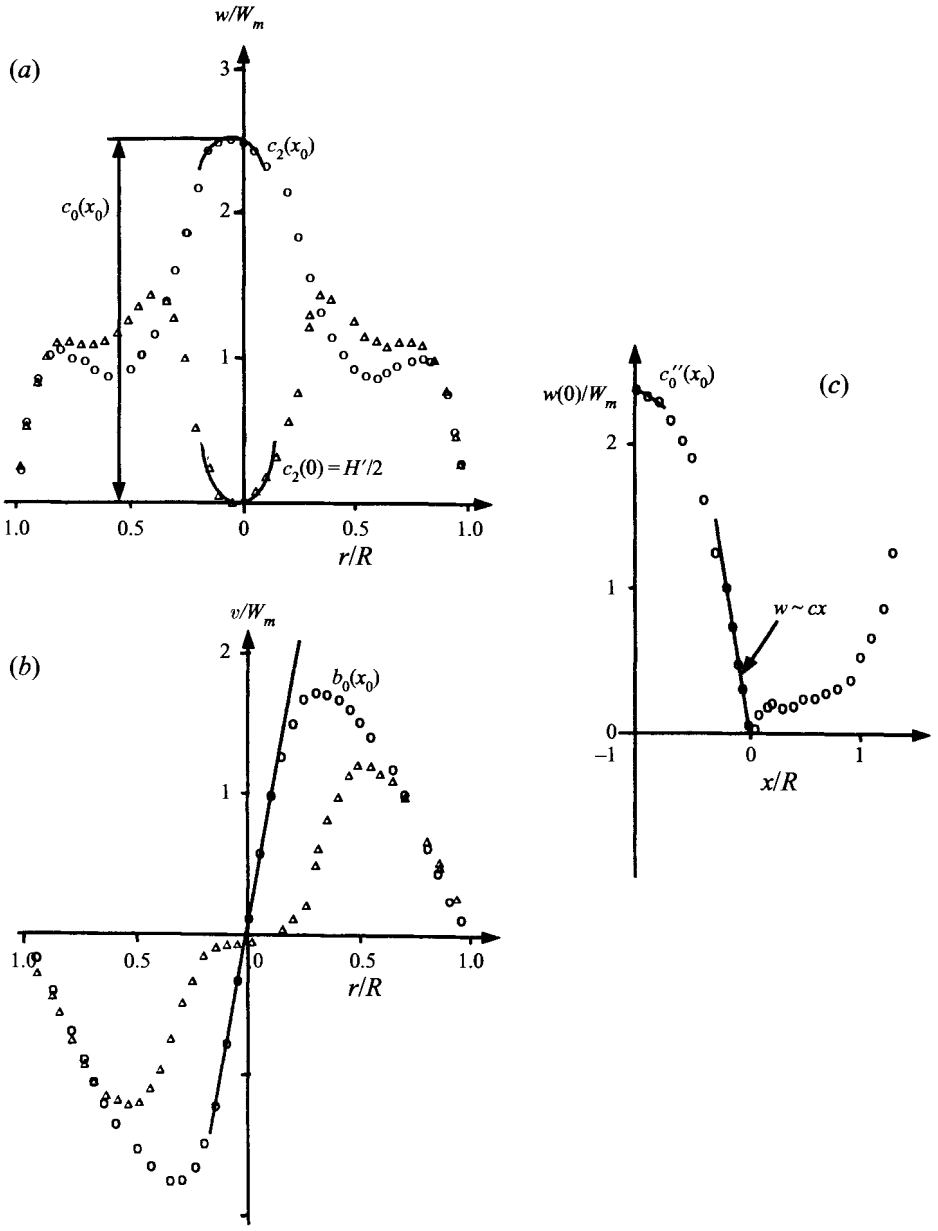

FIGURE 10. Comparison of the present solutions with the experimental data of Uchida *et al.* (1985).

$0 < q < (1+1/\delta)^{1/2}$. Following Leibovich (1984), figure 11 describes this lower-limit line in a q *vs.* $1/\delta$ parameter space. Also shown are the critical line according to Benjamin's (1962) theory, the line for neutral stability of the columnar Q-vortex, $q \approx 1.59$, according to Lessen *et al.*'s (1974) analysis, and (q, δ) values that were fitted by Garg & Leibovich (1979) to experimental inlet flows in pipes that experienced breakdown. It can be seen from figure 11 that all the approach flows in these experiments are supercritical ($N > 1$), stable or marginally stable (according to Lessen *et al.* 1974) ($q > 1.59$) and satisfy the necessary condition $H' > 0$.

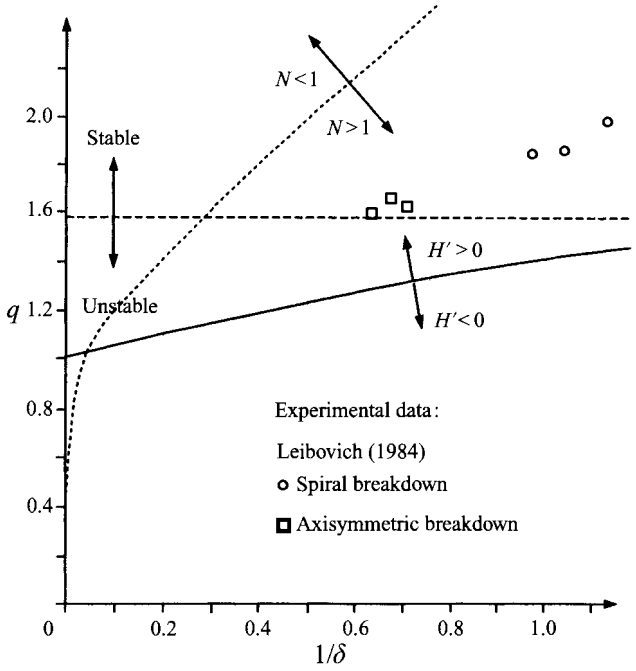

FIGURE 11. Summary of theoretical and experimental results in a q *vs.* $1/\delta$ parameter space: -----, critical line; – – – –, neutral stability line; ——, $H' = 0$ line.

7. Conclusions

The structure of an axisymmetric swirling flow around a vortex breakdown point can be analysed by asymptotic methods. The analysis uses a transformation from the classical Squire–Long equation for the stream function $\psi(x, y)$ to a free boundary problem for the solution of $y(x, \psi)$ for $\psi \geqslant 0$ (outside the bubble). With this approach, we find that there is no need to specify or analyse the nature of the flow inside the bubble. Asymptotic expansions are constructed to describe the approaching swirling flow ahead of the bubble, around the bubble nose and around the separated bubble. The matching processes between those expansions result in two possible solutions. The first solution describes a constant-pressure bubble surface, over which the flow is stagnant. The second solution represents a swirling flow around a pressure-varying bubble surface, where the flow expands along the bubble nose. In both solutions, the bubble nose has a parabolic shape, and both exist only when $H' > 0$ (where H' is the derivative at the vortex centre of the total head H with the stream function ψ, and can be determined from the inlet flow conditions). This result is shown to be equivalent to Brown & Lopez's (1990) criterion for vortex breakdown. It means that the vortex is more receptive to breakdown when the stagnation pressure at the vortex centre is smaller than at its surroundings. Good agreement is found in the region around the stagnation point between the pressure-varying bubble solution and available detailed experimental data for the axisymmetric vortex breakdown.

This research was carried out with the support of the National Science Foundation under Grant CTS-9310181, monitored by Dr S. C. Traugott, Dr R. Powell and Dr D. S. Ahluwalia.

REFERENCES

BATCHELOR, G. K. 1967 *An Introduction to Fluid Dynamics*, pp. 543–545. Cambridge University Press.

BENJAMIN, T. B. 1962 Theory of the vortex breakdown phenomenon. *J. Fluid Mech.* **14**, 593–629.

BERAN, P. S. 1994 The time-asymptotic behavior of vortex breakdown in tubes. *Computers Fluids* **23**, 913–937.

BERAN, P. S. & CULICK, F. E. C. 1992 The role of non-uniqueness in the development of vortex breakdown in tubes. *J. Fluid Mech.* **242**, 491–527.

BERGER, S. A. & ERLEBACHER, G. 1995 Vortex breakdown incipience: theoretical considerations. *Phys. Fluids* **7**, 972–982.

BRAGG, S. L. & HAWTHORNE, W. R. 1950 Some exact solutions of the flow through annular cascade actuator discs. *J. Aero. Sci.* **17**, 243–249.

BREWER, M. 1991 Numerische Losung der Navier–Stokes Gleichungen fur reidimensionale inkompressible instationare Stromungen zur des Wirbelaufplatzens. PhD thesis, RWTH Aachen, Germany.

BROWN, G. L. & LOPEZ, J. M. 1990 Axisymmetric vortex breakdown. Part 2. Physical mechanisms. *J. Fluid Mech.* **221**, 553–576.

BRUECKER, CH. 1995 Development and structural changes of vortex breakdown. *AIAA Paper* 95-2305.

BRUECKER, CH. & ALTHAUS, W. 1992 Study of vortex breakdown by particle tracking velocimetry (PTV), Part I: Bubble type vortex breakdown modes. *Exps. Fluids* **13**, 339–349.

BRUECKER, CH. & ALTHAUS, W. 1995 Study of vortex breakdown by particle tracking velocimetry (PTV), Part 3: Time-dependent structure and development of breakdown modes. *Exps. Fluids* **18**, 174–186.

ESCUDIER, M. P. 1984 Observations of the flow produced in a cylindrical container by a rotating endwall. *Exps. Fluids* **2**, 189–196.

ESCUDIER, M. P. 1988 Vortex breakdown: observations and explanations. *Prog. Aerospace Sci.* **25**, 189–229.

ESCUDIER, M. P. & KELLER, J. J. 1983 Vortex breakdown: a two stage transition. *AGARD CP* 342, pp. 251–258.

FALER, J. H. & LEIBOVICH, S. 1977 Disrupted states of vortex flow and vortex breakdown. *Phys. Fluids* **20**, 1385–1400.

FALER, J. H. & LEIBOVICH, S. 1978 An experimental map of the internal structure of a vortex breakdown. *J. Fluid Mech.* **86**, 313–335.

GARG, A. K. & LEIBOVICH, S. 1979 Spectral characteristics of vortex breakdown. *Phys. Fluids* **22**, 2053–2064.

GOLDSHTIK, M. & HUSSAIN, F. 1992 Inviscid vortical flows with internal stagnation zones. *bull. Am. Phys. Soc. Div. Fluid Dynamics Meeting*, vol. 37, no. 8, p. 1707.

GRABOWSKI, W. J. & BERGER, S. A. 1975 Solutions of the Navier–Stokes equations for vortex breakdown. *J. Fluid Mech.* **75**, 525–544 (and Corrigendum **76**, 1976, 829).

HALL, M. G. 1972 Vortex breakdown. *Ann. Rev. Fluid Mech.* **4**, 195–217.

KELLER, J. J., EGLI, W. & EXLEY, J. 1985 Force- and loss-free transitions between flow states. *Z. Angew. Math. Phys.* **36**, 854–889.

KRIBUS, A. & LEIBOVICH, S. 1994 Instability of strongly nonlinear waves in vortex flows. *J. Fluid Mech.* **269**, 247–264.

LEIBOVICH, S. 1978 The structure of vortex breakdown. *Ann. Rev. Fluid Mech.* **10**, 221–246.

LEIBOVICH, S. 1984 Vortex stability and breakdown: survey and extension. *AIAA J.* **22**, 1192–1206.

LEIBOVICH, S. & KRIBUS, A. 1990 Large amplitude wavetrains and solitary waves in vortices. *J. Fluid Mech.* **216**, 459–504.

LEIBOVICH, S. & STEWARTSON, K. 1983 A sufficient condition for the instability of columnar vortices. *J. Fluid Mech.* **126**, 335–356.

LESSEN, H., SINGH, P. J. & PAILLET, F. 1974 The stability of a trailing line vortex. Part 1. Inviscid theory. *J. Fluid Mech.* **63**, 753–763.

LONG, R. R. 1953 Steady motion around a symmetrical obstacle moving along the axis of a rotating liquid. *J. Met.* **10**, 197–203.

LOPEZ, J. M. 1990 Axisymmetric vortex breakdown. Part 1. Confined swirling flow. *J. Fluid Mech.* **221**, 533–552.

LOPEZ, J. M. 1994 On the bifurcation structure of axisymmetric vortex breakdown in a constricted pipe. *Phys. Fluids* **6**, 3683–3693.

LUNDGREN, T. S. & ASHURST, W. T. 1989 Area varying waves on curved vortex tubes with application to vortex breakdown. *J. Fluid Mech.* **200**, 283–307.

MARSHALL, J. S. 1991 A general theory of curved vortices with circular cross-section and variable core area. *J. Fluid Mech.* **229**, 311–338.

RANDALL, J. D. & LEIBOVICH, S. 1973 The critical state: a trapped wave model of vortex breakdown. *J. Fluid Mech.* **53**, 481–493.

SALAS, M. D. & KURUVILA, G. 1989 Vortex breakdown simulation: a circumspect steady of the steady laminar, axisymmetric model. *Computers Fluids* **17**, 247–262.

SARPKAYA, T. 1971 On stationary and travelling vortex breakdown. *J. Fluid Mech.* **45**, 549–559.

SARPKAYA, T. 1974 Effect of adverse pressure gradient on vortex breakdown. *AIAA J.* **12**, 602–607.

SARPKAYA, T. 1995 Vortex breakdown and turbulence. *AIAA Paper* 95-0433.

SPALL, R. E. & GATSKI, T. B. 1991 A computational study of the topology of vortex breakdown. *Proc. R. Soc. Lond.* A **435**, 321–337.

SPALL, R. E., GATSKI, T. B. & ASH, R. L. 1990 The structure and dynamics of bubble type vortex breakdown. *Proc. R. Soc. Lond.* A **429**, 613–637.

SPALL, R. E., GATSKI, T. B. & GROSCH, C. E. 1987 A criterion for vortex breakdown. *Phys. Fluids* **30**, 3434–3440.

SQUIRE, H. B. 1956 Rotating fluids. In *Surveys in Mechanics* (ed. G. K. Batchelor & R. M. Davies), pp. 139–161. Cambridge University Press.

TRIGUB, V. N. 1985 The problem of breakdown of a line vortex. *Prikl. Math. Mech.* **49**, 166–171.

UCHIDA, S., NAKAMURA, Y. & OHSAWA, M. 1985 Experiments on the axisymmetric vortex breakdown in a swirling air flow. *Trans. Japan Soc. Aeronaut. Space Sci.* **27**, 206–216.